

# **Atomistic Simulation of Mechanical Properties and Fracture Mechanisms in NbSe<sub>2</sub> for Flexible Manufacturing, and Sustainable Engineering Applications**

**Sanjay Kushal Biswas**

Mechanical Engineering Department  
Bangladesh University of Engineering and Technology  
Dhaka, Bangladesh

[Kushal.buet.mechanical.1610072@gmail.com](mailto:Kushal.buet.mechanical.1610072@gmail.com)

**Pratic Sarkar Sourov**

Mechanical Engineering Department  
Bangladesh University of Engineering and Technology  
Dhaka, Bangladesh

[pratic.sarkar.1998@gmail.com](mailto:pratic.sarkar.1998@gmail.com)

**Bishwajit Kar**

Department of Aerospace Engineering and Mechanics  
University of Alabama  
Tuscaloosa, USA  
[bkar@crimson.ua.edu](mailto:bkar@crimson.ua.edu)

## **Abstract**

Two-dimensional (2D) materials such as niobium diselenide (NbSe<sub>2</sub>) are rapidly emerging as promising candidates for next-generation manufacturing due to their exceptional mechanical flexibility, high electrical conductivity, and strong thermal stability. In this study, molecular dynamics (MD) simulations are performed to investigate the tensile properties of monolayer NbSe<sub>2</sub> along the armchair and zigzag configurations throughout a temperature spectrum of 100 K–600 K. The results reveal clear mechanical anisotropy: the zigzag direction consistently shows a higher fracture strain, while Young's modulus and ultimate tensile strength (UTS) exhibit marginal orientation dependence. Increasing temperature leads to noticeable thermal softening, reducing stiffness, UTS, and fracture strain, which are critical for high-temperature device reliability. Beyond their fundamental characterisation, the findings directly facilitate real manufacturing, assembly, and industrial design contexts. The high flexibility and direction-dependent strength of NbSe<sub>2</sub> make it an attractive material for aerospace micro-sensors, vibration-tolerant electronics, soft robotic actuators, flexible wearable sensors, and roll-to-roll printed electronics. The simulation insights support process optimisation, allowing engineers to predetermine safe strain-temperature relationships during fabrication steps for this material, and they also show how atomistic simulation of NbSe<sub>2</sub> can guide material selection, improve production efficiency, and promote sustainable engineering progress.

## **Keywords**

NbSe<sub>2</sub>, Molecular Dynamics Simulation (MD), Anisotropy, Temperature-Dependent Behaviour, Fracture Mechanics

## **1. Introduction**

Graphene and other two-dimensional (2D) compounds known as transition metal dichalcogenides, have garnered significant scientific attention in recent years owing to their distinctive characteristics and promise for transformative technology applications (A. K. Geim, 2009, K. S. Novoselov, 2012, Manish Chhowalla, 2013). TMDCs are interesting because of their diverse structural and electrical properties, like the thermoelectric effect. (Ranjan Kr. Giri, 2023) (Won-Young Lee, 2022) (Min-Sung Kang, 2022) (Ranjan Kr. Giri, 2023), thermal study (Ranjan Kr. Giri, 2021) (Zalak S. Kachhia, 2023) (Priteshkumar M Thakor, 2023), anomalous magnetoresistance (S. Polesya, 2020) (Yangwei Zhang, 2016), superconductivity (Christopher Lane, 20220) (Feng Xiao, 2022), optical study (Shivani Bharucha, 2022) (Ranjan Kr. Giri, 2023), photovoltaic devices (Sayan Roy, 2022) (Hina Pervaiz, 2022) and energy applications (Ranjan Kr. Giri, 2024) (Maitri Patel, 2024), etc. The 2D niobium diselenide ( $\text{NbSe}_2$ ), part of the TMDC family of group V-VI, is getting a lot of attention since it can demonstrate superconductivity at low temperatures (Mohammed S El-Bana, 2013) (Miguel M. Ugeda, 2016) (Xiaoxiang Xi, 2016) (Neal E. Staley, 2009) (R.F. Frindt, 1972). Charge density waves occur from about 33 K in bulk to about 145 K in the monolayer (Miguel M. Ugeda, 2016) (Xiaoxiang Xi, 2015) (I Naik, 2011) (D. J. Huntley, 1976), and the material has great photoconductivity (YH Huang, 2015). Like other TMDCs,  $\text{NbSe}_2$  has a trigonal prismatic crystal structure. The Se-Nb-Se atoms in the plane are strongly covalently bonded, whereas the atoms between layers are weakly bonded by van der Waals forces. This makes it possible to mechanically (Mohammed S El-Bana, 2013) (Neal E. Staley, 2009) (R.F. Frindt, 1972) (Y. Cao, 2015) (K. S. Novoselov, 2005) and chemically (Jonathan N. Coleman, 2011) exfoliate ultrathin sheets. Because of these traits, it is employed in many different ways, including photovoltaic devices (Xin Hu, 2020), (Shivani R. Bharucha, 2023), energy storage (Qingkui Peng, 2021) solid lubricants for sliding contact (Rong Qu, 2021) (Hua Tang, 2011), superconductivity (Haoxiong Zhang, 2022), and more. Because of its high energy storage capacity and rapid charging and discharging rates, it is also an excellent electrode material for sodium-ion (NIB) batteries and lithium-ion (LIB). The reason behind this is that it has low diffusion barriers of 0.086 eV for Na atoms and 0.205 eV for Li atoms, and it absorbs these atoms well (Xingshuai Lv, 2017).

Due to the swift progress in flexible nanoelectronics, TMD materials frequently require folding, bending, or twisting to meet practical applications. Consequently, it is beneficial to examine the mechanical properties of TMDCs to enhance the understanding of their applications. Using traditional molecular dynamics (MD) models, Ding et al. (Wenyang Ding, 2019) examined how h- and t-phase  $\text{WSe}_2$  monolayers in armchair and zigzag orientations were affected by strain rate, temperature, and vacancy defects in terms of tensile strength, fracture strain, and Young's modulus. Their study revealed that h- $\text{WSe}_2$  exhibits significantly higher mechanical strength and stiffness than t- $\text{WSe}_2$ . Increasing temperature led to mechanical performance decline due to enhanced atomic vibrations and stress concentration, whereas influence strain rate has a minimal effect. Jiang et al. (Jin-Wu Jiang, 2013) used the experimental phonon spectra of single-layer  $\text{MoS}_2$  ( $\text{SLMoS}_2$ ) to parameterise a (SW)-Stillinger-Weber potential. To explore how size, chirality, and strain affect the thermal, mechanical properties of  $\text{SLMoS}_2$ , MD simulations were used to take use of this potential. Their findings show that free edges significantly reduce the Young's modulus and thermal stability of  $\text{MoS}_2$  nanoribbons, leading to premature melting below the bulk melting point. Moreover, the study demonstrates that uniaxial tensile strain can effectively tune the thermal conductivity, offering insights into strain engineering of thermal transport in 2D materials. Similarly, Wang et al. (Xinyu Wang, 2019) combined molecular dynamics simulations with machine learning to study the mechanical behaviour of h- $\text{MoSe}_2$  and t- $\text{MoSe}_2$ . They found that h- $\text{MoSe}_2$  is significantly stronger and stiffer than the t-phase, with mechanical properties decreasing as temperature rises. Strain rate had a minor effect. Their machine learning model accurately predicted fracture strength, strain, and Young's modulus, showing the effectiveness of data-driven approaches for evaluating 2D material properties.

The mechanical characteristics of monolayer  $\text{NbSe}_2$  under uniaxial tensile loading in both the zigzag and armchair configurations are investigated in this study using molecular dynamics computational models over a temperature range of 100 K to 600 K. We examine the stress-strain behavior to comprehend the influence of thermal fluctuations on tensile strength, elastic modulus, and fracture strain. Additionally, the fracture mechanics at ambient temperature (300 K) are analyzed in both loading directions to clarify the anisotropic failure mechanisms.

## **2. Methodology**

Molecular dynamics simulations are performed using the Large-scale Atomic/Molecular Massively Parallel Simulator (LAMMPS) program (Aidan P. Thompson, 2022) to investigate the mechanical characteristics of  $\text{NbSe}_2$  under uniaxial tensile stress, with visualisation achieved by the OVITO package (Alexander Stukowski, 2009). The interatomic

interactions within NbSe<sub>2</sub> monolayer are defined by utilizing the Many-body Stillinger-Weber (SW) potentials and parameterized by Jiang et al. To validate the computational process, the Young's modulus of monolayer NbSe<sub>2</sub> is calculated under uniaxial tension load in both armchair and zigzag directions at 300 K and compared with previously reported values from the DFT-based studies, as presented in Table 1.

Table 1: A comparison of the Young's Modulus of h-NbSe<sub>2</sub> derived from this investigation with that reported in existing literature.

| Material          | Armchair Direction |                                  | Zigzag Direction |                                  |
|-------------------|--------------------|----------------------------------|------------------|----------------------------------|
|                   | Calculated (GPa)   | Literature (GPa)                 | Calculated (GPa) | Literature (GPa)                 |
| NbSe <sub>2</sub> | 109.25             | 112 (DFT)<br>(Xingshuai Lv,2017) | 110.33           | 117 (DFT)<br>(Xingshuai Lv,2017) |

## 2.1 Modelling of the structure

The NbSe<sub>2</sub> structure seen in Figure 1 has been generated with Visualization for Electronic and Structural Analysis (VESTA) (Koichi Momma, 2011) and modified by an open-source code in AtomsK (Pierre Hirel, 2015). The lattice constants of h-NbSe<sub>2</sub> is considered 3.48 Å [59]. The AC and ZZ edges are oriented along the x and y directions, respectively. The system dimension of h-NbSe<sub>2</sub> is 95.61×110.4 nm<sup>2</sup> containing 3072 atoms.

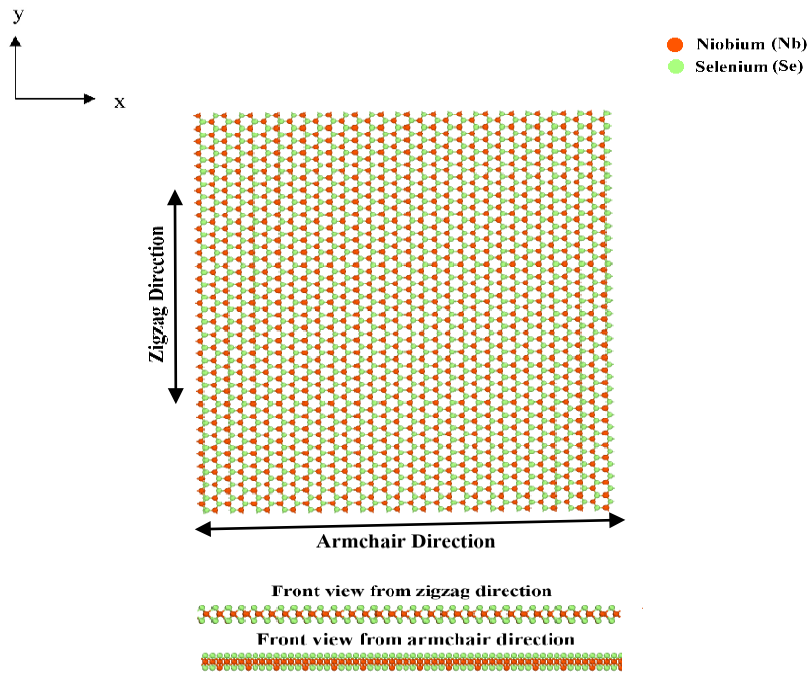


Figure1. Snapshot of the top views of monolayer h-NbSe<sub>2</sub> nanosheet. The armchair and zigzag edges are shown from the side views of the nanosheet.

## 2.2 Tensile Simulations

First, the uniaxial tensile test is carried out using free boundary conditions in the out-of-plane direction and periodic boundary conditions in the in-plane (x and y) directions. Structural stabilization was achieved through energy minimization using the conjugate gradient method (CG). Atomic velocities were given at random using a Gaussian distribution at the designated temperatures. After that, the structure was relaxed to remove any remaining stress in the layers. To reach equilibrium, an NVE ensemble and an NPT ensemble were used for 30 picoseconds each at the ambient pressure and the specified temperature, respectively. To properly equilibrate the structure, the temperature and pressure damping constants were set at 10 femtoseconds. We used a temporal step of one femtosecond in our work. In both armchair and zigzag orientations, the uniaxial tensile strain is applied at a strain rate of 10<sup>9</sup> (s<sup>-1</sup>) at certain

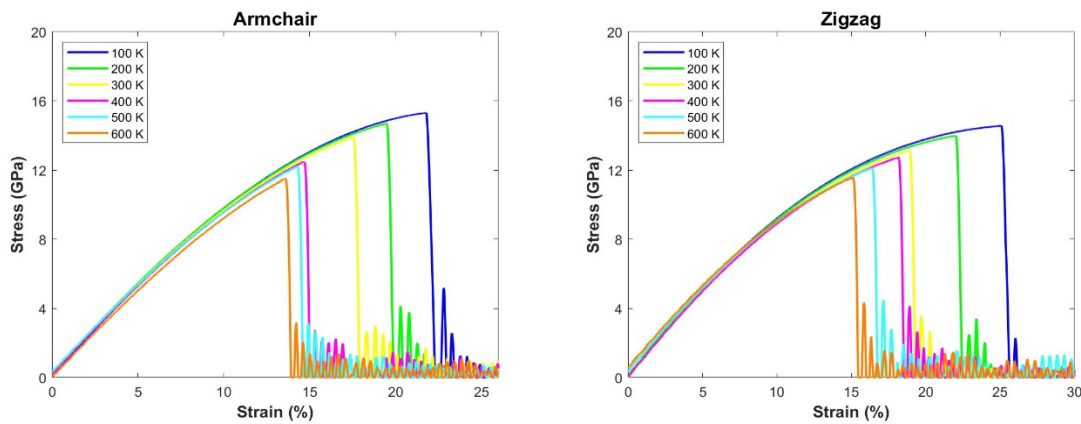
temperatures between 100K and 600K. The main purpose of high strain in this work is to overcome the constraints of length and time scales. Using the virial stress theorem, we calculated the atomic stress (J A Zimmerman, 2004) (Wen Chen, 2006) (Aidan P. Thompson, 2009).

### 3. Result and discussion

The current investigation examines the temperature and chirality-dependent structural characteristics of monolayer h-NbSe<sub>2</sub> by varying the loading direction and temperature. We analysed the strain-stress relationship under uniaxial tensile stress for both the zigzag and armchair directions of NbSe<sub>2</sub> nanosheets across a temperature range of 100K to 600K to understand their influence on mechanical properties and fracture behaviour.

#### 3.1 Chirality and Temperature-dependence of mechanical properties

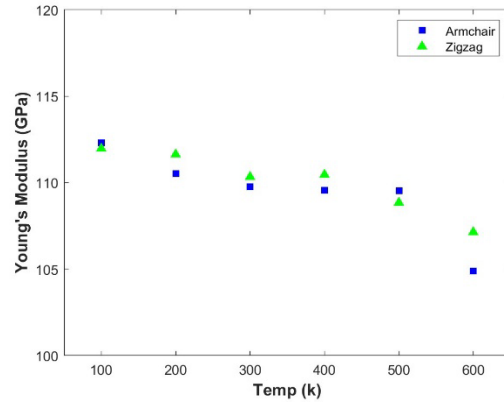
One important characteristic influencing the physical characteristics of two-dimensional (2D) materials is chirality. A major factor affecting atomic energy and mobility is temperature. In this study, we examine the stress-strain behaviour of h-NbSe<sub>2</sub> subjected to uniaxial tensile loading in both the armchair and zigzag orientations. Figure 1 shows the stress-strain curves for both directions.



**Figure 2.** The stress/strain curves of h-NbSe<sub>2</sub> monolayer at different temperatures on (a) armchair loads and (b) zigzag loads.

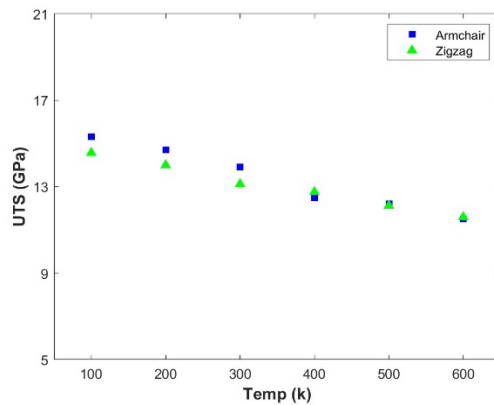
Figures 2(a) and 2(b) illustrate that NbSe<sub>2</sub> exhibits a linear elastic regime during the initial phases of tensile loading, consistent with Hooke's law, whereas in both the armchair and zigzag loading orientations, stress increases as a function of strain. As strain escalates, the curves diverge from linearity, ultimately attaining the ultimate tensile strength (UTS). Following the ultimate tensile strength (UTS) point, a pronounced decline in stress transpires, signifying a brittle fracture process characteristic of transition metal dichalcogenides (TMDs). Figures 2(a) and 2(b) illustrate that the maximum stress in NbSe<sub>2</sub> diminishes as temperature rises for both loading orientations. This trend signifies a decline in the material's strength and rigidity at increased temperatures. Furthermore, the area beneath the stress-strain curve, indicative of the material's toughness, decreases with increasing temperature. This indicates diminished energy absorption capability prior to failure, signifying a decrease in toughness and durability at elevated temperatures. The zigzag orientation permits a somewhat greater fracture strain than the armchair orientation, indicating improved ductility along the zigzag axis.

Moreover, the zigzag direction loading consistently shows a higher ultimate fracture strain than the armchair counterpart across all temperatures, demonstrating the anisotropic mechanical response of NbSe<sub>2</sub>. This can be attributed to the atomic bond orientations present in the armchair and zigzag directions. Structural visualizations of the monolayer under armchair and zigzag loading directions reveal that the atomic bonds are more densely packed in the zigzag orientation. This denser bonding arrangement contributes to higher fracture strain values, resulting in increased resistance to fracture when loaded along the zigzag axis.



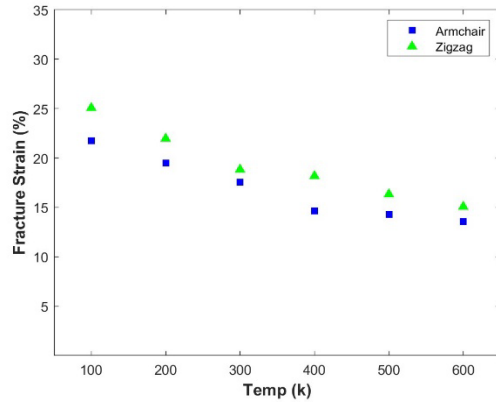
**Figure 3.** Variation of YM of h-NbSe<sub>2</sub> obtained from molecular dynamics simulations conducted at varying temperatures under armchair and zigzag loading conditions.

The variation of Young's modulus (YM) with temperature in both loading directions is shown in Figure 3 for the NbSe<sub>2</sub> monolayer. The results indicate a decreasing trend in Young's modulus as temperature increases. Specifically, in the armchair direction, YM decreases from approximately 112 GPa at 100 K to about 104 GPa at 600 K. In the zigzag direction, it declines from around 112 GPa at 100 K to about 107 GPa at 600 K. Notably, both directions start at the same value (112 GPa) at 100 K. Throughout the temperature range, the zigzag direction generally maintains a slightly higher Young's modulus than the armchair direction.



**Figure 4.** Variation of UTS of h-NbSe<sub>2</sub> obtained from MD simulations with different temperatures under armchair loading and zigzag loading.

Figure 4 presents the variation in ultimate tensile strength (UTS) of the NbSe<sub>2</sub> monolayer under both armchair and zigzag loading across a temperature range of 100K to 600K. As the temperature increases, a clear downward trend in UTS is observed for both loading directions. Initially, from 100 K to 300 K, the armchair orientation maintains slightly higher UTS values compared to the zigzag case. However, with further increase in temperature, the UTS under armchair loading drops more sharply, causing the values for both directions to gradually converge. By 600 K, the difference becomes negligible, suggesting that the influence of loading direction weakens at higher temperatures due to increased thermal activity. In terms of specific values, the UTS in the armchair direction decreases from 15.31 GPa at 100 K to 14.70 GPa at 200 K and 13.91 GPa at 300 K, before falling to 11.52 GPa at 600 K. Meanwhile, the zigzag orientation shows a more gradual decline, with UTS reducing from 14.56 GPa at 100 K to 13.99 GPa, 13.11 GPa, and 11.59 GPa at 200 K, 300 K, and 600 K respectively.

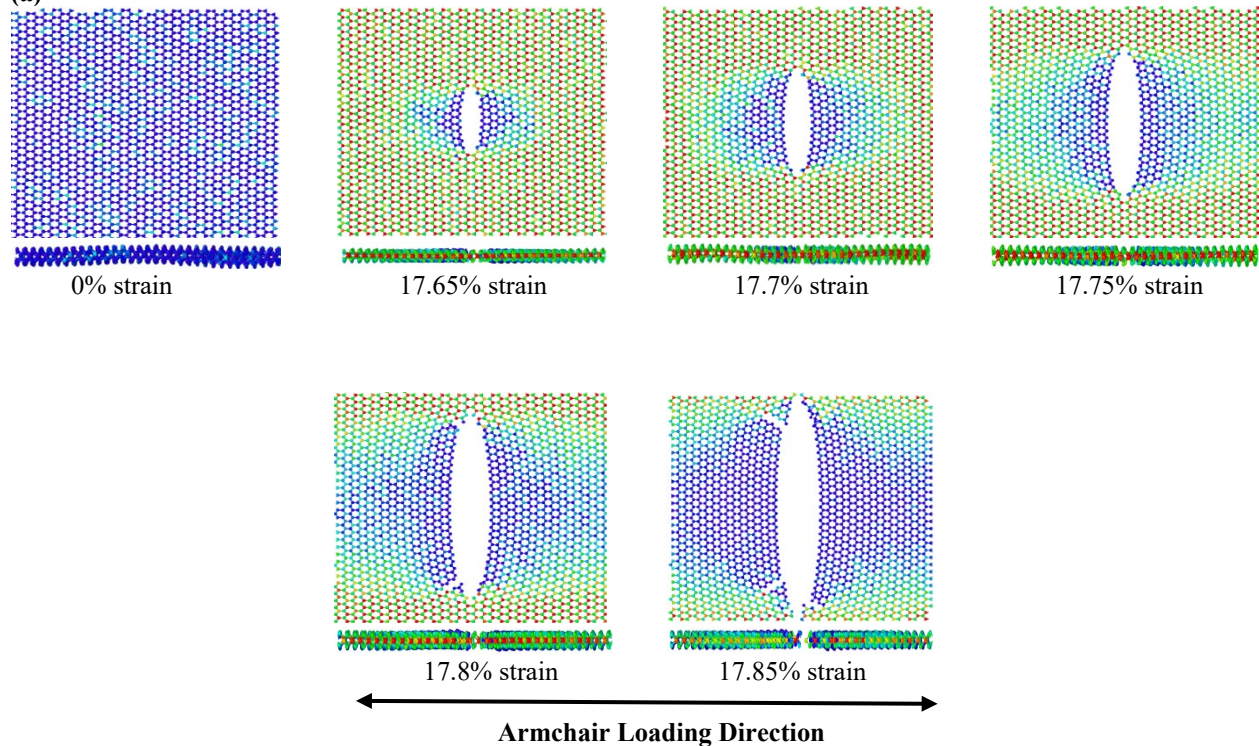


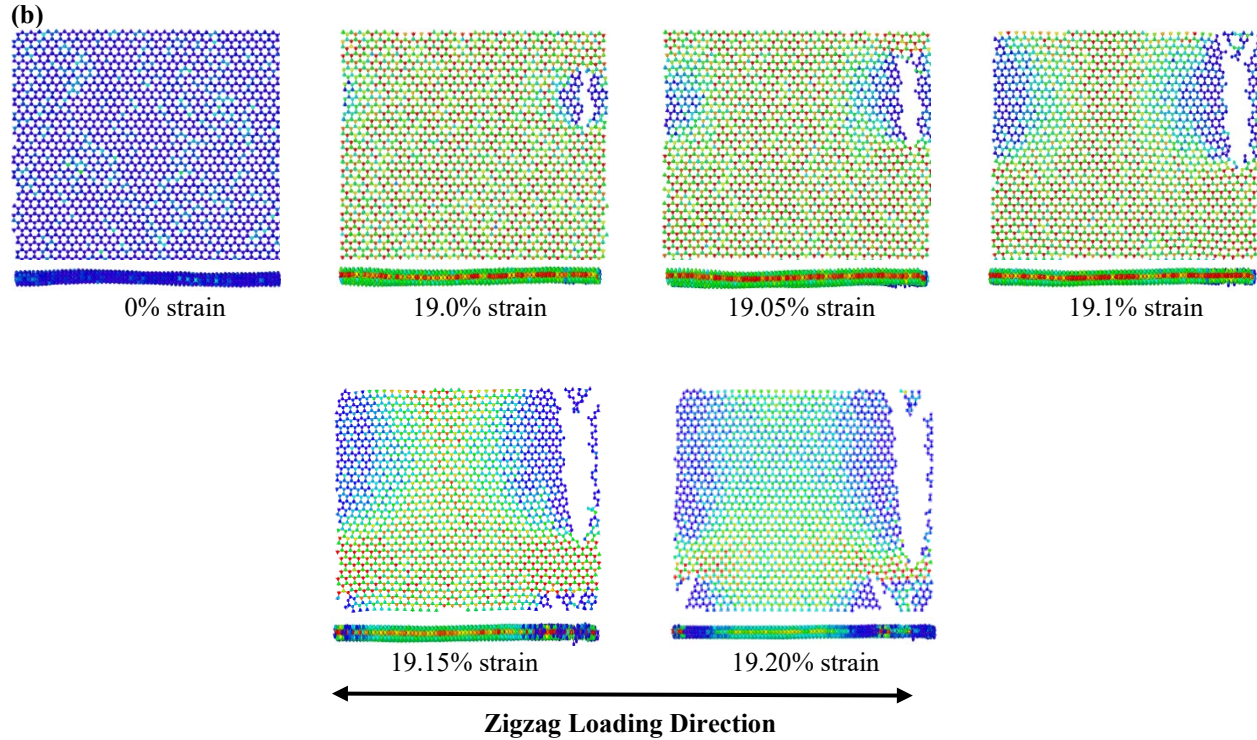
**Figure 5.** Variation of fracture strain of h-NbSe<sub>2</sub> obtained from MD simulations with different temperatures under armchair loading and zigzag loading.

Figure 5 illustrates the variation in fracture strain of the NbSe<sub>2</sub> monolayer under both armchair and zigzag loading across a temperature range of 100K to 600K. Figure 5. Depicts that the armchair direction consistently exhibits lower fracture strain values across the temperature range, dropping from about 22% at 100 K to 16% at 600 K. In contrast, under zigzag loading, the fracture strain decreases from approximately 26% at 100 K to around 17% at 600 K. The fracture strain observed in the zigzag direction is higher likely due to enhanced atomic mobility and a more uniform distribution of strain in this orientation. This trend reflects the anisotropic mechanical behavior of NbSe<sub>2</sub>. The overall reduction in fracture strain with increasing temperature for both directions is consistent with the general thermal softening of materials. At elevated temperatures, increased thermal energy facilitates dislocation motion and reduces the energy barrier for crack propagation, leading to earlier failure and lower fracture strain.

#### Fracture Analysis

(a)





**Figure 6.** Fracture mechanism of NbSe<sub>2</sub> anosheet for different strain values along (a) Armchair loading direction, (b) Zigzag loading direction for 300k temperature.

The fracture mechanisms of monolayer NbSe<sub>2</sub> at 300 K under armchair and zigzag loading orientations are depicted. In Figure 6, red denotes the maximum stress levels, while blue signifies the minimum stress levels. The progression of cracks and fracture patterns are distinctly observable in the front and side view images presented.

Under armchair loading [Figure 6(a)], initial crack occurs at approximately 17.65% strain, followed by rapid crack propagation perpendicular to the loading axis. Complete failure of the nanosheet is observed at a strain of 17.85%. In contrast, under zigzag loading [Figure 6(b)], the crack initiates at around 19% strain due to closely packed bonds in this direction and subsequently propagates along paths inclined at  $\pm 60^\circ$  relative to the loading direction, resulting in full structural rupture at 19.20% strain.

The difference in fracture behavior between the two directions can be attributed to the anisotropic bond orientation within the NbSe<sub>2</sub> lattice. In the armchair direction, bonds are aligned nearly perpendicular to the loading axis, limiting the possibility of crack deflection and promoting a straight crack path. Conversely, in the zigzag configuration, two neighboring bonds at the crack tip are oriented at  $\pm 60^\circ$  to the loading direction, which facilitates crack branching along these angles. Although thermal fluctuations may induce minor branching in both cases, such effects remain limited in the current simulations. This directional dependence of crack propagation is consistent with previous findings in other 2D materials with hexagonal symmetry (Wenyang Ding, 2019) (Emdadul Haque Chowdhury, 2021) (Talukder Musfika Tasnim Oishi, 2021).

#### 4. Conclusion

In this study, we employed molecular dynamics simulations to examine the mechanical characteristics and fracture mechanics of NbSe<sub>2</sub> across a temperature range of 100K to 600K and different loading orientations (armchair and zigzag). Our findings reveal a distinct anisotropic mechanical response between the armchair and zigzag orientations, with the zigzag direction exhibiting higher fracture strain and enhanced ductility across all temperatures. As the temperature increased from 100 K to 600 K, the mechanical properties of h-NbSe<sub>2</sub> showed a clear decline due to thermal softening. Young's modulus decreased from approximately 112 GPa to 104 GPa in the armchair direction and to 107 GPa in the zigzag direction. Similarly, the ultimate tensile strength (UTS) dropped from about 15.31 GPa to 11.52 GPa (armchair) and from 14.56 GPa to 11.59 GPa (zigzag), whereas fracture strain also diminished notably,

from roughly 22% to 14% in the armchair direction and from 25% to 15% in the zigzag direction. The directional dependence of fracture mechanisms further emphasizes the role of lattice orientation in failure behaviour. These insights contribute to a deeper understanding of how chirality and thermal conditions influence the structural resilience of h-NbSe<sub>2</sub>. Our findings not only provide valuable guidelines for the design of defect-tolerant and thermally stable 2D materials but also underscore h-NbSe<sub>2</sub>'s potential for robust performance in next-generation nanoelectronics and energy storage applications. The results directly support actual manufacturing, assembly, and industrial design contexts beyond their basic characterization. NbSe<sub>2</sub>'s great flexibility and direction-dependent strength make it a desirable material for roll-to-roll printed electronics, soft robotic actuators, flexible wearable sensors, vibration-tolerant electronics, and aeronautical microsensors. In addition to demonstrating how atomistic simulation of NbSe<sub>2</sub> can direct material selection, increase production efficiency, and foster sustainable engineering advancement, the simulation insights support process optimization by enabling engineers to predict safe strain-temperature relationships during fabrication steps for this material.

## Reference

- Bharucha, S. R., Dave, M. S., Giri, R. K., Chaki, S. H., & Limbani, T. A., Synthesis of NbSe<sub>2</sub> nanoparticles: An insight into their structural, morphological and optical characteristics, *Engineering Proceedings*, 56(1), 258, 2023.
- Bharucha, S., Dave, M., & Vaidya, R., Electronic and optical studies of NbS<sub>2</sub> semiconductor material, *Materials Today: Proceedings*, 55, 118–121, 2022.
- Cao, Y., Mishchenko, A., Yu, G. L., Khestanova, E., Rooney, A. P., Prestat, E., et al., Quality heterostructures from two-dimensional crystals unstable in air by their assembly in an inert atmosphere, *Nano Letters*, 15(8), 4914–4921, 2015.
- Chen, W., & Fish, J., A mathematical homogenisation perspective of virial stress, *International Journal for Numerical Methods in Engineering*, 67(2), 189–207, 2006.
- Chhowalla, M., Shin, H. S., Eda, G., Li, L. J., Loh, K. P., & Zhang, H., The chemistry of two-dimensional layered transition metal dichalcogenide nanosheets, *Nature Chemistry*, 5(4), 263–275, 2013.
- Chowdhury, E. H., Rahman, M. H., Fatema, S., & Islam, M. M., Investigation of the mechanical properties and fracture mechanisms of graphene/WSe<sub>2</sub> vertical heterostructure: A molecular dynamics study, *Computational Materials Science*, 188, 110231, 2021.
- Coleman, J. N., Lotya, M., O'Neill, A., Bergin, S. D., King, P. J., Khan, U., et al., Two-dimensional nanosheets produced by liquid exfoliation of layered materials, *Science*, 331(6017), 568–571, 2011.
- Ding, W., Han, D., Zhang, J., & Wang, X., Mechanical responses of WSe<sub>2</sub> monolayers: A molecular dynamics study, *Materials Research Express*, 6(8), 085071, 2019.
- El-Bana, M. S., Wolverson, D., Russo, S., Balakrishnan, G., Paul, D. M., & Bending, S. J., Superconductivity in two-dimensional NbSe<sub>2</sub> field effect transistors, *Superconductor Science and Technology*, 26(12), 125020, 2013.
- Frindt, R. F., Superconductivity in ultrathin NbSe<sub>2</sub> layers, *Physical Review Letters*, 28(5), 299, 1972.
- Geim, A. K., Graphene: Status and prospects, *Science*, 324(5934), 1530–1534, 2009.
- Giri, R. K., Chaki, S. H., Dave, M. S., Bharucha, S. R., Khimani, A. J., Kannaujiya, R. M., et al., First-principle insights and experimental investigations of the electronic and optical properties of CuInS<sub>2</sub> single crystals, *Materials Advances*, 4(15), 3246–3256, 2023.
- Giri, R. K., Chaki, S. H., Khimani, A. J., & Deshpande, M. P., Mechanistic insights into transport properties of chemical vapour transport-grown CuInS<sub>2</sub> single crystal, *Journal of Alloys and Compounds*, 959, 170487, 2023.
- Giri, R. K., Chaki, S. H., Khimani, A. J., Patel, S. R., & Deshpande, M. P., Thermal investigation of nanospheres and nanowhiskers of CuInS<sub>2</sub>, *The European Physical Journal Plus*, 136(3), 320, 2021.
- Giri, R. K., Patel, M., Kumar, D., Hmar, J. J. L., Chaki, S. H., Deshpande, M. P., & Kanchan, D. K., CuInS<sub>2</sub> nanospheres and nanowhiskers enhancing the electrochemical properties of sodium-ion-conducting gel polymer electrolytes, *ACS Applied Nano Materials*, 7(3), 2855–2866, 2024.
- Giri, R. K., Solanki, M. B., Chaki, S. H., & Deshpande, M. P., The DFT study of thermoelectric properties of CuInS<sub>2</sub>: A first principle approach, *IOP Conference Series: Materials Science and Engineering*, 1291(1), 012009, 2023.
- Hirel, P., AtomsK: A tool for manipulating and converting atomic data files, *Computer Physics Communications*, 197, 212–219, 2015.
- Hu, X., Xu, E., Xiang, S., Chen, Z., Zhou, X., Wang, N., et al., Synthesis of NbSe<sub>2</sub> single-crystalline nanosheet arrays for UV photodetectors, *CrystEngComm*, 22(35), 5710–5715, 2020.
- Huang, Y. H., Chen, R. S., Zhang, J. R., & Huang, Y. S., Electronic transport in NbSe<sub>2</sub> two-dimensional nanostructures: Semiconducting characteristics and photoconductivity, *Nanoscale*, 7(45), 18964–18970, 2015.
- Huntley, D. J., Charge-density waves and superconductivity in NbSe<sub>2</sub>, *Physical Review Letters*, 36(9), 490, 1976.

- Jiang, J. W., Park, H. S., & Rabczuk, T., Molecular dynamics simulations of single-layer molybdenum disulphide (MoS<sub>2</sub>): Stillinger-Weber parametrisation, mechanical properties, and thermal conductivity, *Journal of Applied Physics*, 114(6), 2013.
- Kachhia, Z. S., Chaki, S. H., Giri, R. K., Parekh, Z. R., Kannaujia, R. M., Hirpara, A. B., et al., Thermal decomposition study of cadmium telluride (CdTe), *Materials Today: Proceedings*, 2023.
- Kang, M. S., Lee, W. Y., Yoon, Y. G., Choi, J. W., Kim, G. S., Kim, S. H., et al., Enhanced transverse Seebeck coefficients in 2D/2D PtSe<sub>2</sub>/MoS<sub>2</sub> heterostructures using wet-transfer stacking, *ACS Applied Materials & Interfaces*, 14(46), 51881–51888, 2022.
- Lane, C., & Zhu, J. X., Identifying topological superconductivity in two-dimensional transition-metal dichalcogenides, *Physical Review Materials*, 6(9), 094001, 2022.
- Lee, W. Y., Kang, M. S., Kim, G. S., Choi, J. W., Park, N. W., Sim, Y., et al., Interface-induced Seebeck effect in PtSe<sub>2</sub>/PtSe<sub>2</sub> van der Waals homostructures, *ACS Nano*, 16(2), 3404–3416, 2022.
- Lv, X., Wei, W., Sun, Q., Huang, B., & Dai, Y., A first-principles study of NbSe<sub>2</sub> monolayer as anode material for rechargeable lithium-ion and sodium-ion batteries, *Journal of Physics D: Applied Physics*, 50(23), 235501, 2017.
- Momma, K., & Izumi, F., VESTA 3 for three-dimensional visualization of crystal, volumetric and morphology data, *Journal of Applied Crystallography*, 44(6), 1272–1276, 2011.
- Naik, I., & Rastogi, A. K., Charge density wave and superconductivity in 2H- and 4H-NbSe<sub>2</sub>: A revisit, *Pramana*, 76(6), 957–963, 2011.
- Novoselov, K. S., Fal'ko, V. I., Colombo, L., Gellert, P. R., Schwab, M. G., & Kim, K., A roadmap for graphene, *Nature*, 490(7419), 192–200, 2012.
- Novoselov, K. S., Jiang, D., Schedin, F., Booth, T. J., Khotkevich, V. V., Morozov, S. V., & Geim, A. K., Two-dimensional atomic crystals, *Proceedings of the National Academy of Sciences*, 102(30), 10451–10453, 2005.
- Oishi, T. M. T., Malakar, P., Islam, M., & Islam, M. M., Atomic-scale perspective of mechanical properties and fracture mechanisms of graphene/WS<sub>2</sub>/graphene heterostructure, *Computational Condensed Matter*, 29, e00612, 2021.
- Patel, M., Giri, R. K., Mishra, K., Chaudhari, J. J., Kanchan, D. K., Singh, P. K., & Kumar, D., Synthesis and assessment of novel Na<sub>2</sub>S-dispersed high-performance nanocomposite gel polymer electrolyte intended for sodium batteries and electric double-layer capacitors, *Journal of Energy Storage*, 86, 111280, 2024.
- Peng, Q., Ling, F., Yang, H., Duan, P., Xu, R., Wang, Q., & Yu, Y., Boosting potassium storage performance via construction of NbSe<sub>2</sub>-based misfit layered chalcogenides, *Energy Storage Materials*, 39, 265–270, 2021.
- Pervaiz, H., Khan, Z. S., Shahzad, N., Ahmed, N., & Jamil, Q., Synthesis and characterisation of CuInS<sub>2</sub> nanostructures and their role in solar cell applications, *Materials Chemistry and Physics*, 290, 126602, 2022.
- Polesya, S., Mankovsky, S., Ebert, H., Naumov, P. G., ElGhazali, M. A., Schnelle, W., et al., Mn<sub>1/4</sub>NbS<sub>2</sub>: Magnetic and magnetotransport properties at ambient pressure and ferro-to-antiferromagnetic transition under pressure, *Physical Review B*, 102(17), 174423, 2020.
- Qu, R., Wen, X., Zhao, Y., Wang, T., Yao, R., & Lu, J., Ultrasonic-assisted top-down preparation of NbSe<sub>2</sub> micro/nanoparticles and hybrid material as a solid lubricant for sliding electrical contact, *Ultrasonics Sonochemistry*, 73, 105491, 2021.
- Roy, S., & Bermel, P., Tungsten-disulphide-based ultrathin solar cells for space applications, *IEEE Journal of Photovoltaics*, 12(5), 1184–1191, 2022.
- Staley, N. E., Wu, J., Eklund, P., Liu, Y., Li, L., & Xu, Z., Electric field effect on superconductivity in atomically thin flakes of NbSe<sub>2</sub>, *Physical Review B*, 80(18), 184505, 2009.
- Stukowski, A., Visualisation and analysis of atomistic simulation data with OVITO – The Open Visualisation Tool, *Modelling and Simulation in Materials Science and Engineering*, 18(1), 015012, 2009.
- Tang, H., Cao, K., Wu, Q., Li, C., Yang, X., & Yan, X., Synthesis and tribological properties of copper matrix solid self-lubricant composites reinforced with NbSe<sub>2</sub> nanoparticles, *Crystal Research and Technology*, 46(2), 195–200, 2011.
- Thakor, P. M., Patel, R. J., Giri, R. K., Chaki, S. H., Khimani, A. J., Vaidya, Y. H., et al., Synthesis, spectral characterisation, thermal investigation, computational studies, molecular docking, and in vitro biological activities of a new Schiff base, *ACS Omega*, 8(36), 33069–33082, 2023.
- Thompson, A. P., Aktulga, H. M., Berger, R., Bolintineanu, D. S., Brown, W. M., Crozier, P. S., et al., LAMMPS – a flexible simulation tool for particle-based materials modelling at the atomic, meso, and continuum scales, *Computer Physics Communications*, 271, 108171, 2022.

- Thompson, A. P., Plimpton, S. J., & Mattson, W., General formulation of pressure and stress tensor for arbitrary many-body interaction potentials under periodic boundary conditions, *The Journal of Chemical Physics*, 131(15), 2009.
- Ugeda, M. M., Bradley, A. J., Zhang, Y., Onishi, S., Chen, Y., Ruan, W., et al., Characterisation of collective ground states in single-layer NbSe<sub>2</sub>, *Nature Physics*, 12(1), 92–97, 2016.
- Wang, X., Hong, Y., Wang, M., Xin, G., Yue, Y., & Zhang, J., Mechanical properties of molybdenum diselenide revealed by molecular dynamics simulation and support vector machine, *Physical Chemistry Chemical Physics*, 21(18), 9159–9167, 2019.
- Xiao, F., Lei, W., Wang, W., Autieri, C., Zheng, X., Ming, X., & Luo, J., Pressure-induced structural transition, metallisation, and topological superconductivity in PdSSe, *Physical Review B*, 105(11), 115110, 2022.
- Xi, X., Wang, Z., Zhao, W., Park, J. H., Law, K. T., Berger, H., et al., Ising pairing in superconducting NbSe<sub>2</sub> atomic layers, *Nature Physics*, 12(2), 139–143, 2016.
- Xi, X., Zhao, L., Wang, Z., Berger, H., Forró, L., Shan, J., & Mak, K. F., Strongly enhanced charge-density-wave order in monolayer NbSe<sub>2</sub>, *Nature Nanotechnology*, 10(9), 765–769, 2015.
- Zhang, Y., Ning, H., Li, Y., Liu, Y., & Wang, J., Negative to positive crossover of the magnetoresistance in layered WS<sub>2</sub>, *Applied Physics Letters*, 108(15), 2016.
- Zhang, H., Rousuli, A., Zhang, K., Luo, L., Guo, C., Cong, X., et al., Tailored Ising superconductivity in intercalated bulk NbSe<sub>2</sub>, *Nature Physics*, 18(12), 1425–1430, 2022.
- Zimmerman, J. A., Webb III, E. B., Hoyt, J. J., Jones, R. E., Klein, P. A., & Bammann, D. J., Calculation of stress in atomistic simulation, *Modelling and Simulation in Materials Science and Engineering*, 12(4), S319, 2004.

## **Biographies**

**Sanjay Kushal Biswas** is a former undergraduate student in the Department of Mechanical Engineering at the Bangladesh University of Engineering and Technology (BUET), Dhaka. His research interests span computational materials science, multiscale modeling, polymer composites, and finite element analysis. He has been working at the Payra Thermal Power Plant—Bangladesh’s largest power plant—for the past 2.5 years. Beyond academics, he is passionate about learning and applying technology to solve real-world challenges. He is currently conducting research in materials engineering, focusing on the analysis of various transition-metal dichalcogenides (TMDs), composites, polymers to enhance production efficiency and support sustainable engineering development.

**Pratic Sarker Sourov** is a former undergraduate student in the Department of Mechanical Engineering at Bangladesh University of Engineering and Technology. His research interests are mainly mechanics of materials, molecular dynamics, materials characterizations, fracture properties and artificial intelligence. He has been working as Assistant Engineer at Gas Transmission Company Limited (GTCL). Beyond academics, he is interested in learning and applying state-of-art methods to solve real-world challenges regarding advanced materials manufacture. He is currently conducting research in materials engineering, focusing on the analysis of various advanced transition-metal dichalcogenides (TMDs), composites, polymers and alloys to enhance production efficiency and support sustainable manufacture.

**Bishwajit Kar** is currently a graduate student at the University of Alabama. He earned his Bachelor of Science in Mechanical Engineering from the Bangladesh University of Engineering and Technology (BUET). His research interests include computational materials science, multiscale modeling, polymer composites, and finite element analysis.